

08,10

## Effect of manganese and silver oxides on the structural and electrochemical properties of polyaniline composites

© I.A. Lobov<sup>1</sup>, S.N. Nesov<sup>1,¶</sup>, E.V. Knyazev<sup>1</sup>, S.A. Matyushenko<sup>1</sup>, K.E. Ivlev<sup>1</sup>,  
E.S. Zemskov<sup>1</sup>, E.A. Grigoriev<sup>2</sup>

<sup>1</sup> Omsk Scientific Center, Siberian Branch, Russian Academy of Sciences,  
Omsk, Russia

<sup>2</sup> St. Petersburg State University,  
St. Petersburg, Russia

¶ E-mail: nesov55@mail.ru

Received November 5, 2025

Revised December 10, 2025

Accepted December 15, 2025

This paper presents an analysis of the structure and electrochemical characteristics of composites obtained by chemical polymerization of aniline in an  $\text{HReO}_4$  solution in the presence of multi-walled carbon nanotubes (MWCNTs) pre-decorated with layers of crystalline  $\text{K}_x\text{MnO}_2$  oxide and non-stoichiometric silver oxide ( $\text{Ag}_{2-x}\text{O}$ ) nanoparticles. The study was conducted using scanning and transmission electron microscopy and cyclic voltammetry. It was shown that the presence of  $\text{K}_x\text{MnO}_2$  oxide on the MWCNT surface ensures the formation of polyaniline (PANI), characterized by a high rate of the leucoemeraldine/emeraldine redox reaction, while the presence of  $\text{Ag}_{2-x}\text{O}$  nanoparticles leads to the formation of hollow PANI microspheres with a diameter of up to  $\sim 500$  nm and a wall thickness of  $\sim 10$  nm. This increases the rate of the n-benzoquinone/hydroquinone redox reaction, which is reflected in an increase in the specific capacitance of the material to 417.1 F/g.

**Keywords:** nanostructured composites, conductive polymers, oxidative polymerization of aniline, metal oxides, electron microscopy.

DOI: 10.61011/PSS.2026.01.63249.312-25

### 1. Introduction

Supercapacitors (SC) are promising power sources for devices that consume energy in a pulsed mode (electronic locks, actuators, radiators, relays, etc.). Compared to electrolytic capacitors, SCs are characterized by a higher capacitance, and also have increased specific power values compared to lithium-ion batteries. Charge accumulation in traditional SC is realized by forming an electrical double layer (EDL) on the surface of porous carbon electrodes placed in an electrolyte, therefore they are often called Electric double-layer capacitors (EDLCs). A significant disadvantage of EDLCs is the low specific energy density, which limits the possibilities of using EDLCs as constant power sources [1–3].

Pseudocapacitors (PC) are a special type of SC in which one or both electrodes contain an active component on the surface of which rapid quasi-reversible redox reactions (or redox reactions) occur during charging/discharging. The capacitance associated with the course of such reactions is commonly referred to as the pseudo-capacitance [4]. In order to increase the surface area on which redox reactions occur, porous and nanostructured materials are used as PC electrode materials. Thus, the accumulation of charge in the EDL also makes a significant contribution to the total capacitance. PCs are characterized by higher values of specific energy and capacitance compared to EDLCs [1]. Transition metal oxides, as well as electrically

conductive polymers, are used as an active component in the composition of PC electrodes [1,4].

Manganese oxide in various forms is the most promising active material for PC due to its high theoretical capacitance, relative environmental safety and accessibility. In addition, manganese oxides doped with alkali metals (K, Na, etc.) have a unique layered structure that allows rapid intercalation of electrolyte ions during the charging process [5–7]. A significant disadvantage of manganese-based oxide systems is their relatively low electrical conductivity, which limits the rate of charge accumulation and recoil. This problem can be solved by adding electrically conductive metals (Ag, Cu, etc.) or their oxides [8,9] to manganese oxide, as well as by forming composites with various carbon materials characterized by a high specific surface area (graphene, carbon nanotubes (CNTs), carbon nanofibers, carbon black) [10,11]. In the latter case, in addition to increasing the electrical conductivity, an increase in the active surface area of the metal oxide is also achieved due to its distribution over the surface of the carbon matrix in the form of layers or nanoparticles.

Polyaniline (PANI) is actively being investigated among electrically conductive polymers as an electrode material for PCs. This polymer can exist in the form of forms with varying degrees of oxidation, the transition between which ensures the accumulation of charge. Despite the high value of the theoretical specific capacitance of PANI (about 2000 F/g) [12], in „pure“ form, it has low plasticity

and mechanical stability, which limits the possibilities of manufacturing SC electrodes based on it. Combining PANI with various types of highly dispersed electrically conductive carbon makes it possible to obtain materials with the necessary set of technological characteristics for the production of PC electrodes, the specific capacitance of which in aqueous inorganic electrolytes is in the range  $10^2 - 10^3$  F/g [13–15].

Of considerable interest is the possibility of creating high-capacitance PC materials based on PANI and manganese oxide [16–18]. In particular, it was reported in Ref. [18] that the composite based on PANI, manganese oxide and Ag nanoparticles has a specific capacitance of over 500 F/g and a high speed capability. The authors explained the high characteristics of the composite by the synergistic effect of combined redox processes involving PANI and manganese oxide, as well as increased electronic conductivity due to the presence of silver nanoparticles.

The structure and electrochemical characteristics of a composite based on multi-walled CNT (MWCNT) and layered oxide  $K_xMnO_2$  doped with nanoparticles of  $Ag_{2-x}O$  were studied in our previous paper [19], the maximum specific capacitance was  $\sim 200$  F/g in an aqueous electrolyte. The possibility of obtaining a material with higher electrochemical characteristics by depositing nanoscale layers of PANI onto the surface of the specified composite is studied in this paper.

## 2. Experiment

### 2.1. Analysis of the structure and composition of composites

The morphology of the composites was studied by scanning electron microscopy (SEM) using a ZEISS MERLIN microscope. The images of the studied samples were obtained in the secondary electron detection mode using a secondary electron energy filter detector for studying nanostructured materials (InLens mode), as well as in the backscattered electron detection mode (AsB mode) for visualizing compositional contrast based on differences in the electron reflection coefficient for the components with different densities. The elemental composition of the materials was studied by energy dispersive X-ray analysis (EDX) using a Jeol JSM-6610 LV scanning electron microscope with an energy dispersive analyzer IncaX-Act at an accelerating voltage of 20 kV.

The structure and morphology of composites were analyzed by transmission electron microscopy (TEM) using Jeol JEM-2100 and Zeiss Libra200FE microscopes in the light-field image mode at an accelerating voltage of 200 kV.

### 2.2. Synthesis of „primary“ composites

In the present work, MWCNT with an average diameter of  $\sim 7-10$  nm, which were synthesized by the method of catalytic gas-phase deposition (MWCNT-1, Institute of

Catalysis of SB RAS, Novosibirsk) were used as the carbon base of composites [20]. The synthesis of „primary“ composites was carried out by treating MWCNT in a solution of  $KMnO_4$  at a temperature of  $60^\circ C$  and with constant stirring.  $AgNO_3$  was added to the reaction solution to dope the composite with silver oxide. The synthesis time of the composites was 6 h. The synthesis conditions were described in detail in our previous work in Ref. [19]. For the sake of brevity, the undoped and doped Ag composites are denoted as K1 and K2, respectively.

### 2.3. Synthesis of composites with PANI

„Primary“ composites K1 and K2 were used as the basis for the formation of composites with PANI, the synthesis of which was carried out by the method of chemical oxidative polymerization of aniline in 1M  $HReO_4$ . Immediately before synthesis, the „primary“ composites were dispersed by ultrasound for 30 min in a solution of rhenium acid. Next, aniline was added to this suspension in an amount of 10 to 1 relative to the „primary“ composite. An aqueous solution of ammonium persulfate (APS) was prepared separately to initiate the polymerization reaction. Aniline and APS were taken in an equimolar ratio. Both solutions were cooled in an ice bath, after which the solution containing APS was added drop by drop to the aniline solution with constant stirring. Next, the solution was stirred at a constant rate at a temperature of  $0^\circ C$  for 1 h. The reaction products were washed with water, ethyl alcohol, and acetone to remove the unreacted components, followed by drying at  $60^\circ C$  and 1 Pa to a constant mass. Composites with PANI obtained on the basis of undoped (K1) and doped Ag (K2) „primary“ composites were designated as P@K1 and P@K2, respectively. According to the described method, a composite based on the initial MWCNT (P@CNT) was also synthesized, which was used as a reference sample in the analysis of electrochemical characteristics.

Traditionally, chemical polymerization of aniline is carried out in the presence of HCl, which is a sufficiently strong acid and can lead to the dissolution of manganese and silver oxides on the surface of MWCNT in „primary“ composites. In view of this, less strong rhenium acid was used when synthesizing composites with PANI instead of hydrochloric acid. The values of the acidity constant index ( $pK_a$ ) for HCl and  $HReO_4$  are  $-5.9$  and  $-1.25$ , respectively. In addition, Re compounds are known for their catalytic activity [21], which can provide a more active interaction of the polymer with metals and their oxides in the formed composites.

### 2.4. Electrochemical analysis of characteristics

The electrodes were formed by pressing the obtained composites with an PANI at a pressure of about 5 MPa without the addition of a binder. The measurements were carried out by cyclic voltammetry (CV) using a three-electrode circuit with a platinum counterelectrode and a Ag/AgCl reference electrode in a 1M HCl electrolyte. To

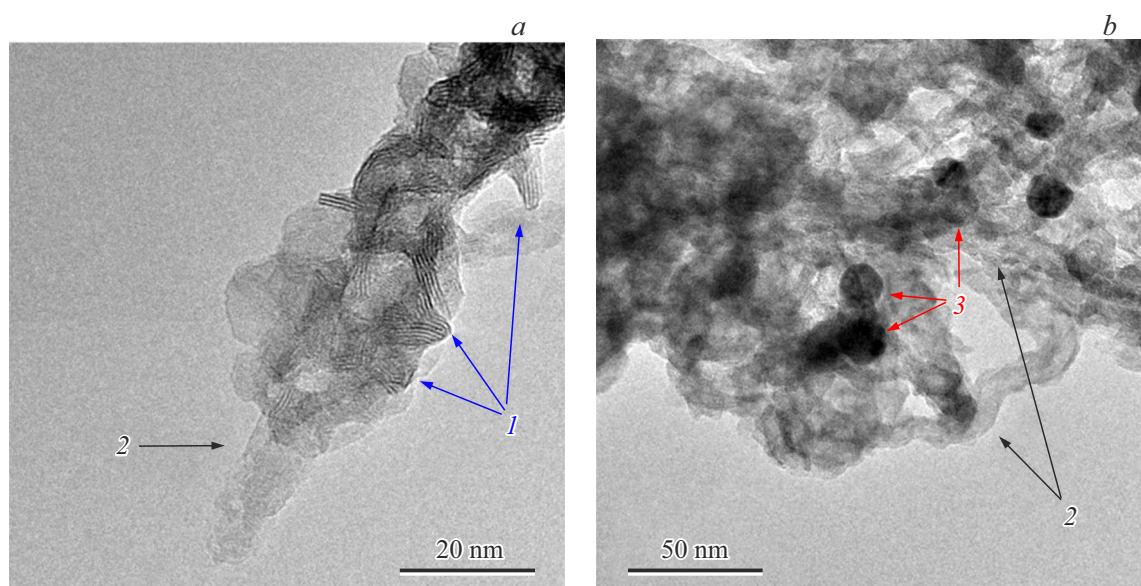


**Figure 1.** TEM images of composites K1 (*a*) and K2 (*b*). Designations: 1 — crystallites  $K_xMnO_2$ ; 2 — MWCNT coated with  $K_xMnO_2$ ; 3 — nanoparticles  $Ag_{2-x}O$ .

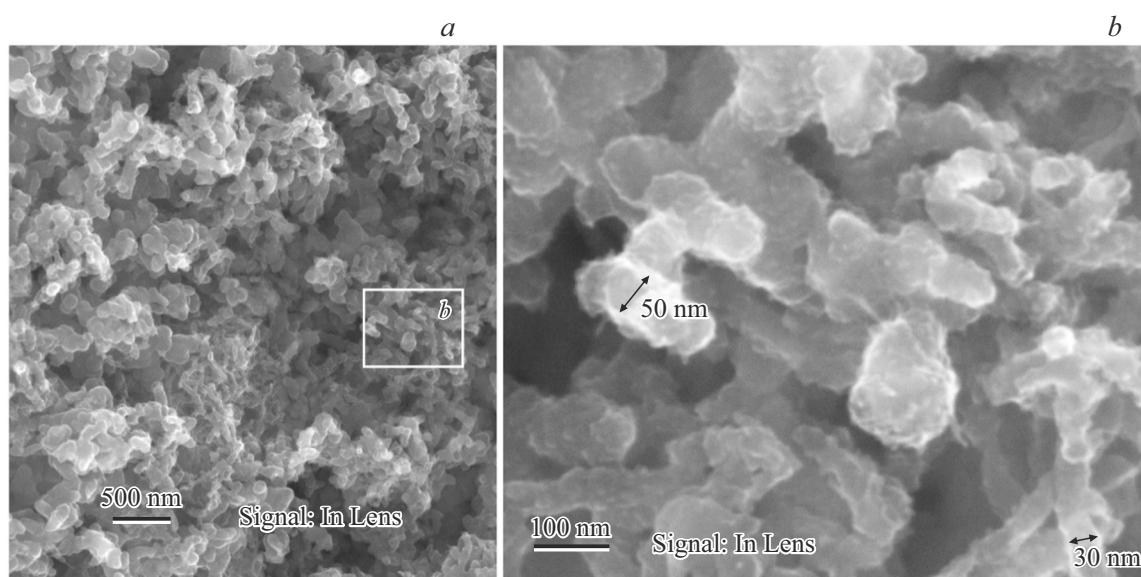


**Figure 2.** SEM images of the P@K1 composite obtained in the mode „InLens“.

determine the specific capacitance, CV data was used in the potential range from 0 to 0.8 V at a potential expansion rate from 1 to 10 mV/s. When calculating the electrochemical characteristics, the energy conversion method was used [22].

### 3. Results and discussion

#### 3.1. Structure and composition of composites

The MWCNT surface in the „primary“ K1 composite (Figure 1, *a*) is covered with crystallites, which were previously identified using a complex of methods as crystallites

of  $K_xMnO_2$  [19]. The K2 composite has a similar structure, however, it additionally contains nanoparticles of nonstoichiometric oxide  $Ag_{2-x}O$  with characteristic sizes up to  $\sim 15$  nm (Figure 1, *b*). The silver content in the K2 composite according to X-ray photoelectron spectroscopy is  $\sim 1$  at.% [19].

Analysis of a series of SEM images of the P@K1 composite showed that it has a homogeneous morphology (see Figure 2). The presence of tubular structures with a characteristic diameter up to  $\sim 50$  nm, which are obviously MWCNT, the surface of which is covered with a layer of

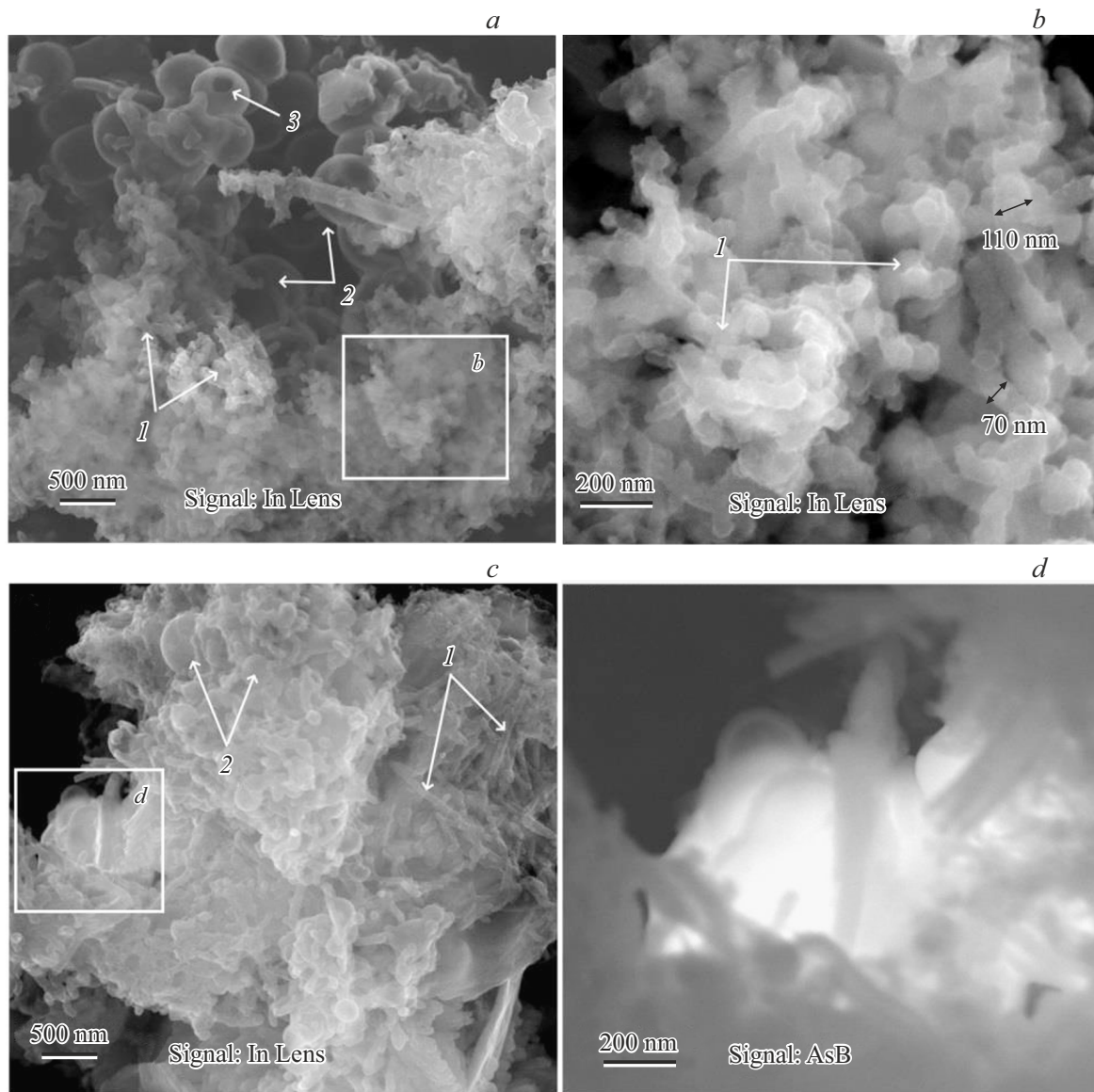


**Figure 3.** SEM images of the P@K2 composite obtained in the „InLens“ (*a–c*) and „AsB“ (*d*) modes. Designations: 1 — tubular structures (MWCNT covered with PANI); 2 — microspheres; 3 — hole in the microsphere wall.

PANI. Estimated thickness of PANI layer reaches  $\sim 20$  nm. There are no polymer-uncoated MWCNT in the composite.

Analysis of the SEM images of the P@K2 composite showed that its morphology is heterogeneous (Figure 3). There are two types of structural formations. The first type comprises tubular structures similar to those present in the P@K1 composite. An assessment of the characteristic sizes of tubular structures (up to  $\sim 110$  nm) suggests that the thickness of the PANI layers in the composite P@K2 on the MWCNT surface reaches  $\sim 50$  nm. The second type of structural formations present in the composite P@K2 comprises sphere-like structures (microspheres), the characteristic diameter of which is in the range of  $\sim 200$ – $500$  nm (Figure 3). Some of these microspheres have clearly distinguishable holes with diameters from several tens to  $\sim 100$  nm, through which their hollow

structure is visible (Figure 3, *a*). The higher brightness of the microspheres compared to the tubular structures in the SEM images obtained in the „AsB“ mode (Figure 3, *d*) suggests a higher polymer density in the microspheres. This may be due to its doping with silver or its compounds. Formation of similar spherical formations during synthesis of PANI in the presence of metals (Ag, Au) is described in the literature [23,24]. However, the mechanisms of growth of PANI hollow spherical structures remain unexplored.

The results obtained at five different sites with a size of  $200 \times 200 \mu\text{m}$  were averaged to compare the quantitative elemental composition of composites using the EDX method. Typical spectra of P@K1 and P@K2 composites are shown in Figure 4, *a* and Figure 4, *b*, respectively. It was found that there is no manganese and potassium in

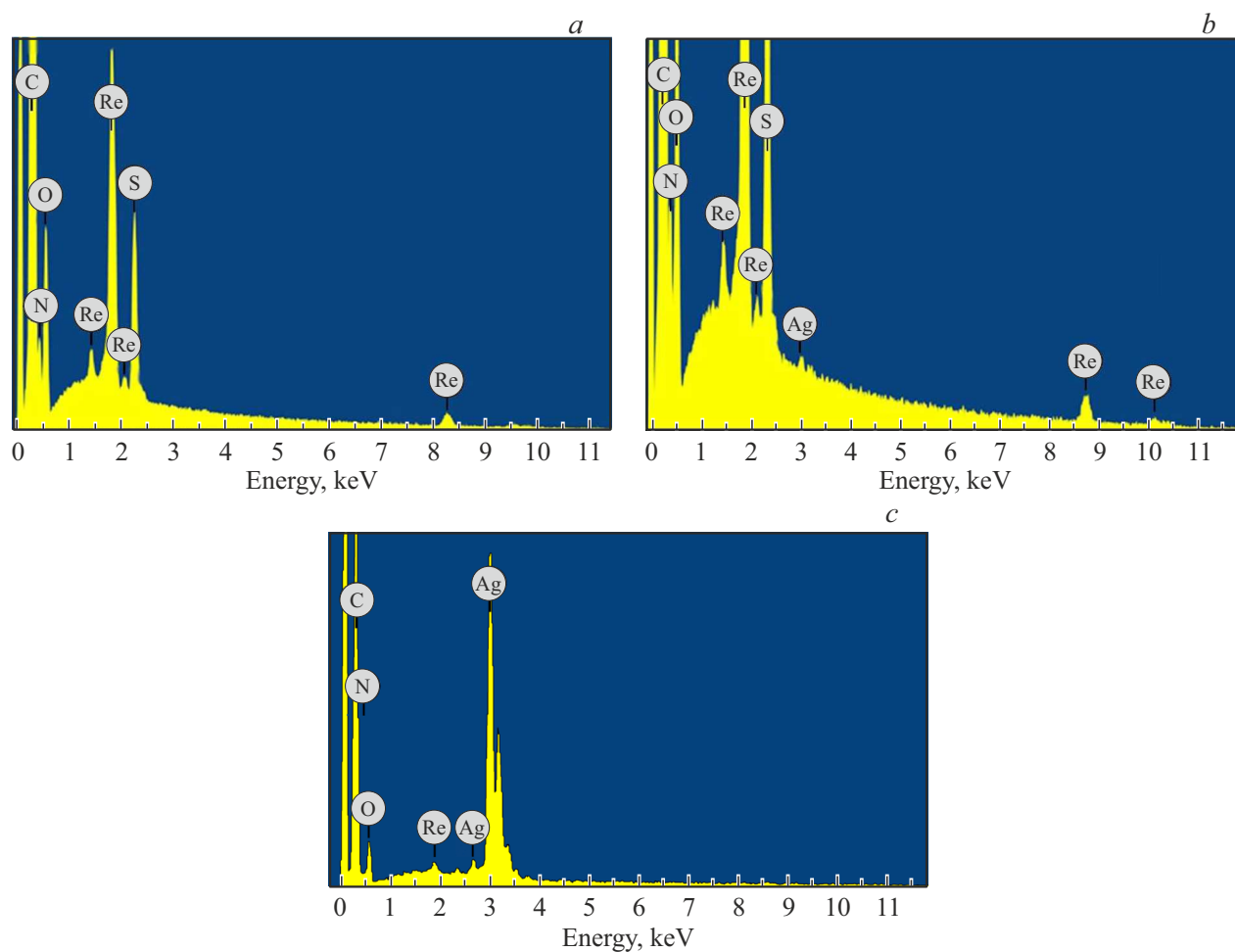


**Figure 4.** EDX spectra of composites P@K1 (a) and P@K2 (b), measured in areas of size  $200 \times 200 \mu\text{m}$  and EDX spectrum of composite P@K2 (c), measured at a point containing a cluster of microspheres (the area shown in Figure 3, d).

Composite composition according to EDX data (average value for 5 sites)

Composite	Concentration, at.%					
	C	N	O	S	Re	Ag
P@K1	$75.9 \pm 0.86$	$13.5 \pm 0.62$	$8.4 \pm 0.28$	$1.1 \pm 0.05$	$1.1 \pm 0.05$	–
P@K2	$75.8 \pm 2.79$	$13.0 \pm 1.48$	$8.4 \pm 2.84$	$1.2 \pm 0.41$	$0.9 \pm 0.17$	$0.7 \pm 0.22$

both composites with PANI (Figure 4, a and Figure 4, b, table). This indicates the dissolution of the oxide  $\text{K}_x\text{MnO}_2$  present on the surface of MWCNT in „primary“ composites during the polymerization of aniline. The EDX spectra of the P@K2 composite contain Ag lines (Figure 4, b and Figure 4, c), the average concentration of which is  $\sim 0.7$  at.% (table). At the same time, the intensity of Ag lines in the EDX spectra for areas with a cluster of microspheres is significantly higher (Figure 4, c). Based on the presented results, it can be argued that it is the nanoparticles of nonstoichiometric oxide  $\text{Ag}_{2-x}\text{O}$  present in the „primary“ K2 composite that can be the centers of formation of microspheres in the composite P@K2.

The ratio of carbon and nitrogen concentrations in P@K1 and P@K2 composites is typical for PANI. The Re present in both composites indicates the doping of the polymer with rhenium acid. The presence of sulfur and oxygen is associated with the residues of the reaction products of ammonium persulfate used in the polymerization of aniline as an oxidizer [15].

The analysis of the TEM images showed that the P@K1 composite contains a PANI layer formed on the surface of the MWCNT has a homogeneous amorphous structure and does not contain dense nanoparticles (Figure 5). It is clearly seen that  $\text{K}_x\text{MnO}_2$  crystallites are also absent on the surface of the MWCNT (Figure 5, c). This confirms

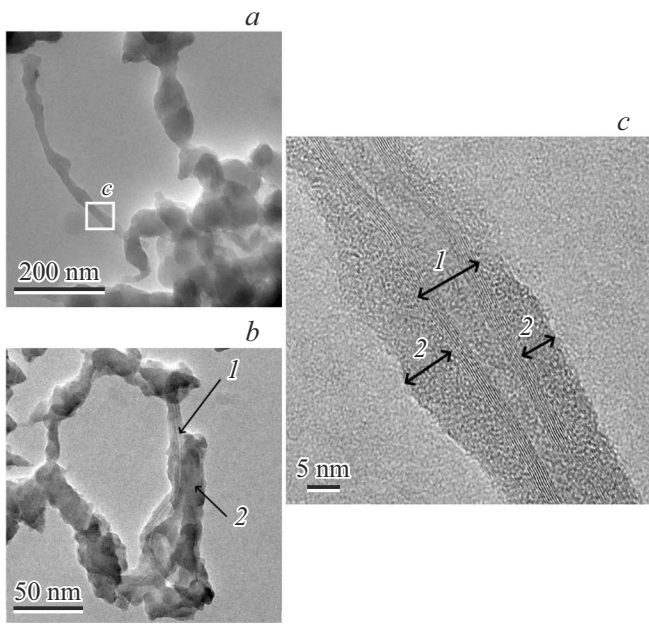


**Figure 5.** TEM images of the P@K1 composite at various magnifications. Designations: 1 — MWCNT; 2 — PANI layer.

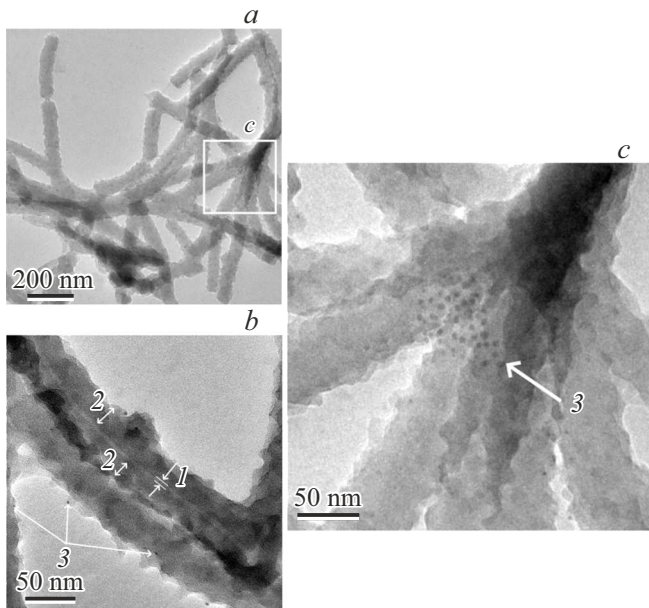


**Figure 6.** TEM images of tubular structures in the composite P@K2. Designations: 1 — MWCNT; 2 — PANI layer; 3 — dense nanoparticles

the complete dissolution of  $K_xMnO_2$  crystallites during the polymerization of aniline.

The analysis of TEM images of tubular structures in the P@K2 composite (Figure 6) suggests that in this case there are PANI layers on the surface of the MWCNT with a higher thickness (compared to P@K1 composite). Typical thickness of PANI layer is  $\sim 20\text{--}30$  nm. In the thickness of the polymer layer, the presence of fragmentarily distributed

dense nanoparticles with sizes of the order of several nm is observed (Figure 6, c), which, according to EDX data, most likely contain silver atoms.

Analysis of TEM images of microspheres present in the P@K2 composite confirms the presence of internal cavities in them (Figure 7). According to our estimates, the wall thickness of the microspheres is  $\sim 10$  nm. The observed contrast differences on the walls of the spheres can be related both to fluctuations in the thickness of the polymer layer and to local differences in their structure and composition. Clusters of dense nanoparticles are present on some sections of the microsphere walls (Figure 7, c), which presumably contain silver atoms. The individual microspheres in the TEM images are not completely closed (Figure 7, b).

The obtained data on the structure and composition of composites with PANI (P@K1 and P@K2) showed that, contrary to our expectations, the oxide  $K_xMnO_2$  present on the surface of the MWCNT in „primary“ composites turned out to be unstable under the conditions of polymerization of aniline using rhenium acid. The EDX method did not detect the presence of manganese and potassium atoms in the P@K1 and P@K2 composites. We believe that the oxide  $K_xMnO_2$  in an acidic environment can also participate as an aniline oxidizer in the process of oxidative polymerization, which, in turn, can significantly affect the PANI electrochemical activity. It is shown that the presence of nanoparticles of nonstoichiometric silver oxide in the primary K2 composite leads to the formation of hollow PANI microspheres with diameters up to  $\sim 500$  nm and wall thickness of  $\sim 10$  nm.

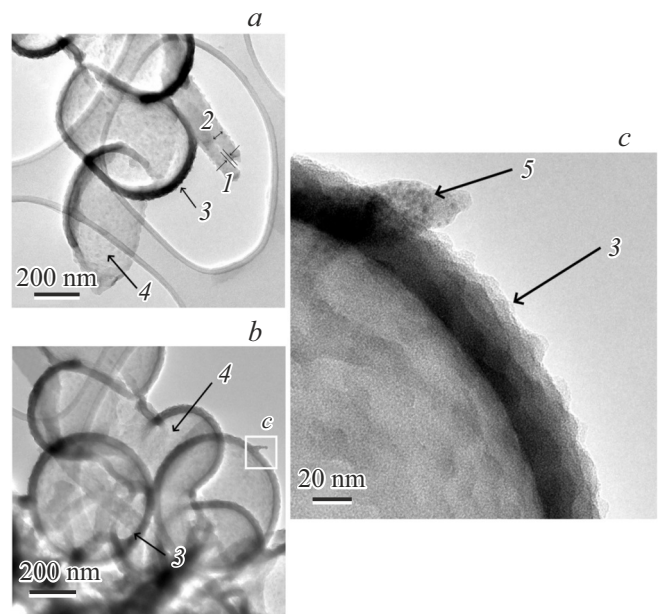


**Figure 7.** TEM image of microspheres in the P@K2 composite. Designations: 1 — MWCNT; 2 — PANI layer on the MWCNT; 3 — microspheres; 4 — microspheres with holes in the walls; 5 — dense nanoparticles.

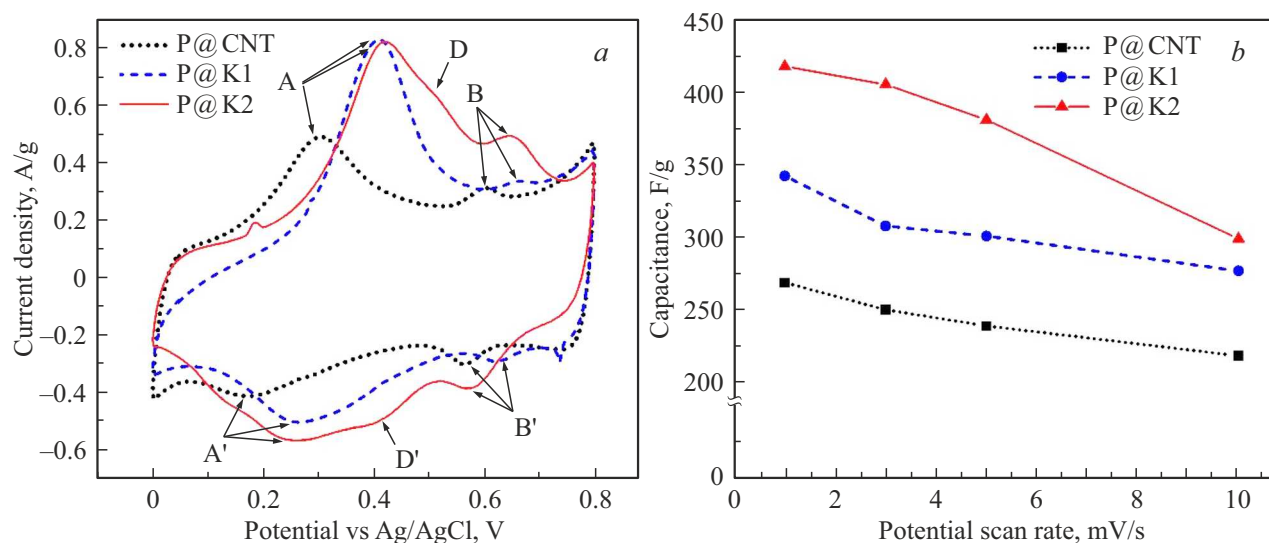


**Figure 8.** *a* — cyclic voltammogram of composites, measured at a potential scan rate of 1 mV/s; *b* — dependence of the specific capacitance of composites on the scan rate.

### 3.2. Electrochemical characteristics of composites

Cyclic voltammogram of all composites are typical for PANI redox peaks A/A' and B/B', corresponding to the leucoemeraldine/emeraldine transformations and the formation of the n-benzoquinone/hydroquinone pair, respectively [15,25,26] (Figure 8, *a*). However, on cyclic voltammogram of P@K1 and P@K2 composites, these peaks are shifted to the region of high potential values (the shift is  $\sim 100$  and  $50$  mV for peaks A/A' and B/B', respectively), which indicates an increase in the potential of these reactions compared to the P@CNT composite. This may be due to the more oxidized form of PANI synthesized in the presence of MWCNT coated with a layer of  $K_xMnO_2$ .

At the same time, the peak values of the current density for the oxidation reaction A is almost twice as high for P@K1 and P@K2 composites compared to the P@CNT composite, which indicates a significant increase in the rate of leucoemeraldine oxidation. Since the values of the potential of the redox reaction A/A', as well as the peak values of the current density of this reaction for composites P@K1 and P@K2 practically coincide, we believe that these changes in electrochemical behavior may be attributable to the influence of oxide  $K_xMnO_2$ , which is present on the MWCNT surface in both „primary“ composites, on the PANI structure. This oxide in an acidic environment can participate in the oxidation reaction of aniline with reduction to a highly soluble oxide  $Mn^{2+}$ . This assumption is consistent with the absence of manganese in the results of elemental analysis of P@K1 and P@K2 composites.

The peak A has a noticeable extended „shoulder“ on the CV curve of the P@K2 composite in the region of high potential values, denoted as D (Figure 8, *a*). We believe that this peak may also be responsible for the leucoemeraldine oxidation reaction that occurs on the

surface of polymer microspheres present in the P@K2 composite. The increase in the reaction potential in this case may be due to a higher electrical contact resistance at the „sphere–sphere“ boundary compared to the „layer of PANI-MWCNT surface“ contact resistance. The oxidative peak B on the voltammogram of the P@K2 composite is characterized by a higher peak current density and is located in a wider potential range. This may also be attributable to the difference in the oxidation reaction potential of n-benzoquinone on the surface of the tubular and spherical structures present in the composite. At the same time, the high peak current density for peak B indicates an increase in the oxidation rate of n-benzoquinone in the P@K2 composite compared to the P@K1 composite. We believe that the latter may be attributable to the effect of dimensionality, namely, the nanoscale thickness of the PANI in the walls of microspheres. We showed earlier in Ref. [15] that the formation of nanoscale layers of PANI leads to a significant increase in the rate of the redox reaction n-benzoquinone/hydroquinone.

The dependences of the specific capacitance ( $C_s$ ) on the potential scan rate for the studied electrodes are shown in Figure 8, *b*. It can be seen that the  $C_s$  values for the electrodes based on P@K1 and P@K2 are significantly higher compared to the electrode based on P@CNT. The electrode based on P@K2 has the maximum specific capacitance ( $C_s = 417.1$  F/g at a potential scan rate of 1 mV/s). The rapid decrease in specific capacitance for all electrodes is due to the high contribution of redox processes to charge accumulation.

## 4. Conclusion

This paper studied the possibility of synthesizing nanostructured composite materials based on PANI and MWCNT,

decorated with layers of crystalline oxide  $K_xMnO_2$  and nanoparticles of  $Ag_{2-x}O$ , the structure and electrochemical properties of the obtained materials were analyzed. Aniline was polymerized using rhenium acid as a dopant in the synthesis of composites. The analysis of the elemental composition of the obtained composites by the EDX method did not reveal the presence of manganese or potassium in their composition. However, an analysis of the electrochemical characteristics showed an increase in the rate of the leucoemeraldine/emeraldine redox reaction in a polymer formed on the surface of MWCNT pre-decorated with  $K_xMnO_2$  oxide. Presumably,  $K_xMnO_2$  oxide can act as an additional aniline oxidizer during polymerization. The presence of  $Ag_{2-x}O$  nanoparticles leads to the formation of supramolecular structural PANI formations in the composite in the form of hollow microspheres with a wall thickness of  $\sim 10$  nm. According to SEM the PANI in the composition of the walls of microspheres has a high density and contains inclusions of nanoparticles containing Ag. Analysis of cyclic voltammogram showed that the presence of microspheres provides a significant increase in the electrochemical activity of the material due to an increase in the rate of the n-benzoquinone/hydroquinone redox reaction. Analysis of electrochemical characteristics of the obtained composites with PANI showed that the pre-decoration of the MWCNT surface with  $K_xMnO_2$  oxide ensures an increase in the maximum specific capacitance of composites by 27%. Additional doping of the primary “composite with  $Ag_{2-x}O$  nanoparticles ensures an increase in the maximum specific capacitance by  $\sim 55\%$ .

## Acknowledgments

The SEM research was conducted on a non-financial basis using the equipment of the Resource Center „Nanotechnology“ of St. Petersburg State University (project AAAAA-A19–119091190094). The TEM studies were conducted using the equipment of the Omsk Regional Center for Collective Use of the Siberian Branch of the Russian Academy of Sciences.

## Funding

The study was performed under framework of State Assignment of Omsk Scientific center of Siberian Branch of Russian Academy of Science (state registration number of project 121021600004-7).

## Conflict of interest

The authors declare that they have no conflict of interest.

## References

- [1] Yu.M. Volkovich. *Elektrokhimiya* **57**, 4, 197 (2021) (in Russian). DOI: 10.31857/S0424857021040101
- [2] M.E. Şahin, F. Blaabjerg, A. Sangwongwanich. *Energies* **15**, 3, 674 (2022). <https://doi.org/10.3390/en15030674>
- [3] M. Pershaanaa, Shahid Bashir, S. Ramesh, K. Ramesh. *J. Energy Storage* **50**, 104599 (2022). <https://doi.org/10.1016/j.est.2022.104599>
- [4] T. Prasankumar, J. Jose, S. Jose, S.P. Balakrishnan. In: *Supercapacitors for the Next Generation*. IntechOpen (2022). p. 154. DOI: 10.5772/intechopen.98600
- [5] M. Moharramnejad, A. Ehsani, R.E. Malekshah, M. Shahi, R. Bavandpour, H. Rajabi, S.M. Mojab. *J. Mater. Sci.: Mater. Electron.* **33**, 19693 (2022). <https://doi.org/10.1007/s10854-022-08828-z>
- [6] E.A. Arkhipova, A.S. Ivanov, S.K. Nikolenko, K.I. Maslakov, S.V. Savilov, S.M. Aldoshin. *Zhurnal prikladnoi khimii* **96**, 1, 4 (2023) (in Russian). DOI: 10.31857/S0044461823010012
- [7] S.N. Nesov, I.A. Lobov, S.A. Matyushenko, E.A. Grigoriev. *ECS J. Solid State Sci. Technol.* **13**, 101002 (2024). DOI: 10.1149/2162-8777/ad8517
- [8] M.U. Khalid, S. Zulfiqar, M.N. Khan, I. Shakir, M.F. Warsi, E.W. Cochran. *Mater. Adv.* **5**, 15, 6170 (2024). <https://doi.org/10.1039/d4ma00118d>
- [9] R. Ai, X. Zhang, S. Li, Z. Wei, G. Chen, F. Du. *Chem. Eur. J.* **30**, e202400791 (2024). DOI: 10.1002/chem.202400791
- [10] L. Chen, Y. Zhang, C. Hao, X. Zheng, Q. Sun, Y. Wei, B. Li, L. Ci, J. Wei. *ChemElectroChem* **9**, e202200059 (2022). DOI: 10.1002/celec.202200059
- [11] Z. Pan, C. Yang, Y. Li, X. Hu, X. Ji. *Chem. Eng. J.* **428**, 131138 (2022). DOI: 10.1016/j.cej.2021.131138
- [12] H. Li, J. Wang, Q. Chu, Z. Wang, F. Zhang, S. Wang. *J. Power Sources* **190**, 2, 578 (2009). DOI: 10.1016/j.jpowsour.2009.01.052
- [13] H. Yu, G. Xin, X. Ge, C. Bulin, R. Li, R. Xing, B. Zhang. *Compos. Sci. Technol.* **154**, 76 (2018). <https://doi.org/10.1016/j.compscitech.2017.11.010>
- [14] E.I. Yesilyurt, J. Pionteck, F. Simon, B. Voit. *RSC Appl. Polym.* **1**, 97 (2023). <https://doi.org/10.1039/D3LP00061C>
- [15] I.A. Lobov, S.N. Nesov, E.A. Drozdova. *FTT* **66**, 9, 1591 (2024) (in Russian). DOI: 10.61011/FTT.2024.09.58785.188
- [16] S. Xi, X. Qian, X. Cheng, H. Liu, H. Shabanzadeh, D. Dastan. *iScience* **28**, 2, 111774 (2025). <https://doi.org/10.1016/j.isci.2025.111774>
- [17] S. Abbas, S. Manzoor, M. Abdullah, et al. *J. Mater. Sci.: Mater. Electron.* **33**, 25355 (2022). <https://doi.org/10.1007/s10854-022-09242-1>
- [18] C. Pan, Y. Lv, H. Gong, Q. Jiang, S. Miao, J. Liu. *RSC Adv.* **6**, 21, 17415 (2016). <https://doi.org/10.1039/c5ra18403g>
- [19] S.N. Nesov, I.A. Lobov, S.A. Matyushenko, E.V. Knyazev, V.V. Bolotov, E.S. Zemskov, E.V. Zhizhin, A.V. Koroleva, E.A. Grigoriev. *FTT* **67**, 6, 1010 (2025) (in Russian). DOI: 10.61011/FTT.2025.06.60949.154-25
- [20] V.L. Kuznetsov, D.V. Krasnikov, A.N. Schmakov, K.V. Elumeeva. *Phys. Status Solidi B* **249**, 12, 2390 (2012). DOI: 10.1002/pssb.201200120
- [21] A. Olding, M. Tang, C.C. Ho, R.O. Fuller, A.C. Bissember. *Dalton Trans.* **51**, 8, 3004 (2022). <https://doi.org/10.1039/d1dt04205j>
- [22] S.A. Matyushenko, S.N. Nesov. *Dinamika sistem, mekhanizmov i mashin* **12**, 78 (2024) (in Russian).
- [23] N.M. Farrage, A.H. Oraby, E.M.M. Abdelrazek, D. Atta. *Biointerface Res. Appl. Chem.* **9**, 3, 3934 (2019). <https://doi.org/10.33263/BRIAC93.934941>

- [24] S. Abdulla, J. Dhakshanamoorthi, V.P. Dinesh, B. Pullithadathil. *J. Biosens. Bioelectron* **6**, 2 (2015). DOI: 10.4172/2155-6210.1000165
- [25] I.V. Panasenko, M.O. Bulavskiy, A.A. Iurchenkova, Y. Aguilar-Martinez, F.S. Fedorov, E.O. Fedorovskaya, B. Mikladal, T. Kallio, A.G. Nasibulin. *J. Power Sources* **541**, 231691 (2022). DOI: 10.1016/j.jpowsour.2022.231691
- [26] L. Sun, D. Miyagi, Y. Cai, A. Ullah, M.K. Haider, C. Zhu, M. Gopiraman, I.S. Kim. *J. Energy Storage* **61**, 106738 (2023). DOI: 10.1016/j.est.2023.106738

*Translated by A.Akhtyamov*